



The TRiC/CCT Chaperone Is Implicated in Alzheimer's Disease Based on Patient GWAS and an RNAi Screen in A β -Expressing *Caenorhabditis elegans*

Eleonora Khabirova^{1,2,3}, Aileen Moloney^{1,3,4,5,9}, Stefan J. Marciniak^{3,7}, Julie Williams⁸, David A. Lomas¹⁰, Stephen G. Oliver^{6*}, Giorgio Favrin^{6†}, David B. Sattelle^{4,9†}, Damian C. Crowther^{1,3,*†}

1 Department of Genetics, University of Cambridge, Cambridge, United Kingdom, **2** Department of Biochemistry, University of Cambridge, Cambridge, United Kingdom, **3** Cambridge Institute for Medical Research, University of Cambridge, Cambridge, United Kingdom, **4** MRC Functional Genomics Unit, Department of Physiology, Anatomy and Genetics, University of Oxford, Oxford, United Kingdom, **5** Sir William Dunn School of Pathology, University of Oxford, Oxford, United Kingdom, **6** Cambridge Systems Biology Centre, University of Cambridge, Cambridge, United Kingdom, **7** Department of Medicine, University of Cambridge, Cambridge, United Kingdom, **8** Department of Psychiatry and Neurology, MRC Centre for Neuropsychiatric Genetics, Cardiff University School of Medicine, Cardiff, United Kingdom, **9** The Wolfson Institute for Biomedical Research, University College London, London, United Kingdom, **10** Department of Medicine, University College London, London, United Kingdom

Abstract

The human A β peptide causes progressive paralysis when expressed in the muscles of the nematode worm, *C. elegans*. We have exploited this model of A β toxicity by carrying out an RNAi screen to identify genes whose reduced expression modifies the severity of this locomotor phenotype. Our initial finding was that none of the human orthologues of these worm genes is identical with the genome-wide significant GWAS genes reported to date (the “white zone”); moreover there was no identity between worm screen hits and the longer list of GWAS genes which included those with borderline levels of significance (the “grey zone”). This indicates that A β toxicity should not be considered as equivalent to sporadic AD. To increase the sensitivity of our analysis, we then considered the physical interactors (+1 interactome) of the products of the genes in both the worm and the white+grey zone lists. When we consider these worm and GWAS gene lists we find that 4 of the 60 worm genes have a +1 interactome overlap that is larger than expected by chance. Two of these genes form a chaperonin complex, the third is closely associated with this complex and the fourth gene codes for actin, the major substrate of the same chaperonin.

Citation: Khabirova E, Moloney A, Marciniak SJ, Williams J, Lomas DA, et al. (2014) The TRiC/CCT Chaperone Is Implicated in Alzheimer's Disease Based on Patient GWAS and an RNAi Screen in A β -Expressing *Caenorhabditis elegans*. PLoS ONE 9(7): e102985. doi:10.1371/journal.pone.0102985

Editor: Koichi M. Iijima, National Center for Geriatrics and Gerontology, Japan

Received: February 5, 2014; **Accepted:** June 25, 2014; **Published:** July 31, 2014

Copyright: © 2014 Khabirova et al. This is an open-access article distributed under the terms of the Creative Commons Attribution License, which permits unrestricted use, distribution, and reproduction in any medium, provided the original author and source are credited.

Funding: The funders had no role in study design, data collection and analysis, decision to publish, or preparation of the manuscript. AM & JW were supported by Alzheimer's Research UK (<http://www.alzheimersresearchuk.org>). DCC was supported by an Alzheimer's Research UK Senior Research Fellowship (<http://www.alzheimersresearchuk.org>, grant code: ART-SRF2010-2) and the MRC (<http://www.mrc.ac.uk>) and EPSRC (<http://www.epsrc.ac.uk/>), UK (grant code: G0700990). SJM is supported by the MRC, UK (<http://www.mrc.ac.uk>, grant code: G0601840). JW was supported by the MRC, UK (<http://www.mrc.ac.uk>, grant codes: G0300429 and G0902227) and the Wellcome Trust (<http://www.wellcome.ac.uk>, grant code: 082604/2/07/Z). DAL was supported by the MRC, UK (<http://www.mrc.ac.uk>, grant code: G0901786) and the NIHR UCLH BRC (<http://www.uclhospitals.brc.nihr.ac.uk>). DCC, DAL, GF, and SGO are all co-investigators on the Wellcome Trust/MRC Neurodegenerative Diseases Research Initiative (<http://www.wellcome.ac.uk>, grant code: WT089703AIA).

Competing Interests: The authors have declared that no competing interests exist.

* Email: steve.oliver@bioc.cam.ac.uk (SGO); dcc26@cam.ac.uk (DCC)

† These authors contributed equally to this work.

‡ These authors also contributed equally to this work.

Background

Once age is taken into account, the most powerful determinants of risk for Alzheimer's disease (AD) are genetic; indeed, the heritability of the disorder is estimated to be 58–79% [2,3]. In the clinic however, this strong genetic influence is not readily apparent because of the heterogeneous, multigenic inheritance of so-called sporadic AD. Such complexity has encouraged geneticists to focus on a small minority of AD cases that exhibit dominant Mendelian inheritance [4,5]. Remarkably, these studies have shown that the bulk of the genetic lesions resulting in familial AD (FAD) directly influence the proteolytic processing of a single transmembrane protein called amyloid precursor protein (APP) [6]. The cleavage of APP by β -secretase and then γ -secretase results in the generation of a spectrum of peptides, known as amyloid β (A β),

that are the major component of senile plaques in the brains of patients with AD. The γ -secretase is of particular interest because its cleavage of APP determines which amino acids constitute the C-terminus of A β . Normally, A β peptides are predominantly 40 amino acids in length (A β_{40}), while 5–10% have a further 2 amino acids at the C-terminus (A β_{42}). The bulk of cases of FAD can be accounted for by mutations that either increase the total amount of A β [7,8], or favour the production of longer, more aggregation-prone, isoforms of the peptide [9]. FAD has been reported to be a consequence of variation in the sequence or copy number of either the APP gene, or the genes PSEN1 or PSEN2 encoding catalytic subunits of γ -secretase [7,8]. Likewise, protection from AD has also been linked to a polymorphism in APP that interferes with β -secretase cleavage [10]. These data, supported by studies on sporadic AD patients [11], have given rise to the amyloid cascade

hypothesis that places the aggregation of A β as the first step on the road to AD [6].

The advent of genome-wide association studies (GWAS) has made the investigation of multigenic disorders, such as sporadic AD, experimentally tractable. Using $p < 10^{-7}$ as an empirical cut off for genome-wide significance (the GWAS “white zone”), the first generation of multicentre AD GWAS [12,13] reported four genes (*apoE*, *clusterin*, *PICALM*, and *CRI*) associated with disease risk. With the publication of the second generation of GWAS findings, the total number of risk genes is now twenty one [1,14]. Notable absentees from these lists are any of the genes implicated in FAD. These findings may lead us to question the relevance of A β in the pathogenesis of sporadic AD and might indicate that the sporadic and familial forms are different diseases.

One explanation for the absence of genes such as *APP*, *PSEN1*, or *PSEN2* from the list of candidates identified by GWAS is that the studies were lacking sufficient power to detect small or rare contributions to risk [15]. Increased power could be achieved by recruiting more patients and controls and by increasing the density of SNP genotyping [15]. However, we have taken a parallel approach by including in our analysis not only the genes with genome-wide significance (GWAS “white zone”), but also GWAS results of borderline significance (GWAS “grey zone”) with p -values between $< 10^{-5}$. This larger list of genes will include false positives, that can safely be ignored, but equally there will be genes that carry risk and are involved in the pathogenesis of sporadic AD. Our approach has been to probe this larger group of GWAS white+grey zone genes using the results of a genome-scale screen in a model system that reports exclusively on the toxicity of the A β peptide. We postulate that if A β toxicity were distinct from sporadic AD then we would expect to see an overlap between the worm and human genes lists that is consistent with chance. However were the GWAS data reporting a role for A β in clinical AD we would expect to see a significantly increased overlap in the network of genes identified in the human and worm screens.

Results

Feeding RNAi to *C. elegans* modifies the A β -induced paralysis phenotype

We identified 7970 human protein-encoding genes that have orthologues in *C. elegans* and we used a subset of the Ahringer *C. elegans* RNAi library [16] to systematically knock down the transcript levels of each of these genes. The phenotypic consequences of each genetic knock-down were assessed in worms following the induction of A β expression under the control of a heat-inducible myocyte-specific promoter. The optimal age for A β induction was 48 h (stage L3) because this resulted in 50% paralysis 30 h later (Fig. S1). Induction of A β expression in younger worms resulted in a more rapid progression of paralysis. Rigorous primary and secondary screens identified RNAi clones that significantly ($p < 0.05$, $n = 12$ with 4 biological replicates) enhanced or suppressed the A β -induced paralysis phenotype. Clones that modified paralysis were positively identified by DNA sequencing. In this way, we identified 78 worm genes that significantly suppressed (Table 1) the A β -induced paralysis phenotype. Of the 3 genes that significantly enhanced the phenotype none has a human orthologue (Table 2).

Human orthologues of worm screen hits are not identical to GWAS genes but are network hubs

In our initial analysis, we generated a list of the human orthologues of the worm modifier genes using EnsemblCompara [17], and found that 61 out of the 78 worm genes had human

counterparts. This ratio is significantly higher than one would expect by chance if one considers that there are only 7,970 worm genes that have human orthologues out of a genome of approximately 20,000 genes [18]. The p -value for this enrichment is $p < 10^{-11}$ (binomial test using probability of success = 7970/20000, number of successes = 61, number of trials = 78), indicating that the hits in the worm screen are much more likely to have human orthologues than one would expect by chance.

Using worm ontology enrichment analysis (clueGO plugin for Cytoscape) we found that a number of labels were over-represented in our screen hits, implicating genes involved in ATP synthesis, purine metabolism, protein binding and chaperone activity, and components of the translational machinery (Table 3).

When we compared this list of 61 human orthologues of the worm modifier genes with the 63 genes in the GWAS white+grey zone (Table S1) we found no identity between the two gene lists. Indeed when we compared the ontology labels associated with the GWAS genes and the human orthologues of worm screen hits we found that there was no significant similarity (using WEB-based GENE SeT AnaLysis Toolkit, bioinfo.vanderbilt.edu/webgestalt/). However using the BioGrid database (v. 3.2.96) [19] we found that 6 of the human orthologues of worm screen genes coded for proteins that interact directly with the products of the GWAS white+grey zone genes.

In order to determine which, if any, of the worm screen hits interacted with the GWAS list to a statistically significant degree we supplemented the candidate gene lists with genes encoding the first-degree physical interactors (+1 interactome) of the protein products of the primary members using the BioGrid database (v. 3.2.96). We then asked, for each member of the worm-screen hit list, whether their +1 interactome overlap with GWAS was greater, or less, than one would expect by chance (Fig. S2). Of the 61 worm genes, 60 were present in the Biogrid database and we considered these further in our analysis. Of the 63 genes in the GWAS white+grey zone, 52 were present in Biogrid database.

It was immediately apparent from the relative sizes of the +1 interactomes (Figs. 1 & 2) that the genes derived from the worm screen were more highly interacting than the GWAS list. Specifically each worm screen gene orthologue had, on average, 53 interactors as compared to the GWAS list where the value was less than 14.

Ranking the distribution of gene interconnectivity

In order to determine whether the observed bias towards highly interconnected genes in the worm modifier list was statistically significant, we used a computational approach to compare our observed population of genes to similar, randomly generated, lists. Firstly we ranked the population of human genes in the Biogrid database (13940 genes) according to their number of interactors. This ranked list was then divided into 10 bins such that each bin contained the same number of human orthologues of worm genes (that is 797 in each bin). For example, this resulted in the most highly interconnected 952 human genes in the database being put into the first bin; the bin boundaries for the whole database were: 1–952, 953–2006, 2007–3175, 3176–4403, 4404–5735, 5736–7134, 7135–8624, 8624–10200, 10201–12104 and 12105–13928. Using a Monte-Carlo approach [20] we then generated 100 lists containing 60 randomly generated human genes with worm orthologues.

As expected the genes in the random lists segregated with equal frequency into the various bins (Fig. 3, triangles); however, a consequence of the highly interconnected nature of the worm screen gene list is that >50% of its members (31 out of 60) fall within the most highly interconnected bin on the left side of graph.

Table 1. Suppressors of the A β -paralysis phenotype.

| <i>C. elegans</i> gene symbol | Human gene name | Human gene symbol | Accession number |
|-------------------------------|--|-------------------|------------------|
| F46E10.1 | Long chain fatty acid acyl-CoA ligase | ACSF2 | NM_001028767 |
| T04C12.6 | Actin and related proteins | ACTB | NM_073416 |
| T25C8.2 | Actin and related proteins | ACTG1 | NM_067408 |
| K07C5.1 | Actin-related protein Arp2/3 complex, subunit Arp2 | ACTR2 | NM_073256 |
| F55A12.7 | AP-1 complex subunit mu-1 | AP1M1 | NM_059171 |
| F29G9.3 | Clathrin adaptor complex, small subunit | AP1S2 | NM_072158 |
| C13B9.3 | Medium subunit of clathrin adaptor complex | ARCN1 | NM_066062 |
| C34E10.6 | F0F1-type ATP synthase, beta subunit | ATP5B | NM_065710 |
| R10E11.8 | Vacuolar H ⁺ -ATPase V0 sector, subunits c/c' | ATP6V0C | NM_066764 |
| Y49A3A.2 | Vacuolar H ⁺ -ATPase V1 sector, subunit A | ATP6V1A | NM_074158 |
| F20B6.2 | Vacuolar H ⁺ -ATPase V1 sector, subunit B | ATP6V1B2 | NM_076310 |
| Y55F3AR.3 | Chaperonin complex component, TCP-1 theta subunit (CCT8) | CCT8 | NM_067634 |
| F09G2.4 | mRNA cleavage and polyadenylation factor II complex, subunit CFT2 (CPSF subunit) | CPSF2 | NM_072421 |
| M03F8.3 | Cell cycle control protein (crooked neck) | CRNKL1 | NM_001129507 |
| B0464.1 | Aspartyl-tRNA synthetase | DARS | NM_066688 |
| C55B6.2 | dsRNA-activated protein kinase inhibitor P58, contains TPR and DnaJ domains | DNAJC3 | NM_076808 |
| D2085.3 | Translation initiation factor 2B, epsilon subunit (eIF-2Bepsilon/GCD6) | EIF2B5 | NM_063440 |
| F22B5.2 | Translation initiation factor 3, subunit g (eIF-3g) | EIF3G | NM_001276737 |
| C40H1.4 | Elongation of very long chain fatty acids protein 3 | ELOVL3 | NM_066655 |
| H19N07.1 | Eukaryotic Peptide Chain Release Factor | GSPT2 | NM_001269363 |
| T10C6.11 | Histone H2B | HIST1H2BA | NM_074630 |
| F26D10.3 | Molecular chaperones HSP70/HSC70, HSP70 superfamily | HSPA8 | NM_070667 |
| C49F5.1 | S-adenosylmethionine synthetase | MAT1A | NM_077601 |
| C30A5.3 | MOB-Like Protein Phocein | MOB4 | NM_066397 |
| Y57G11C.12 | NADH:ubiquinone oxidoreductase, NDUFA6/B14 subunit | NDUFA6 | NM_070389 |
| K07C5.4 | Ribosome biogenesis protein - Nop56p/Sik1p | NOP56 | NM_073259 |
| T22B11.5 | 2-oxoglutarate dehydrogenase, E1 subunit | OGDHL | NM_068216 |
| D1054.15 | Isoform 1 of Pleiotropic regulator 1 | PLRG1 | NM_001269330 |
| F36A4.7 | RNA polymerase II, large subunit | POLR2A | NM_068122 |
| K02B12.3 | Prolactin regulatory element binding | PREB | NM_059904 |
| R07E4.6 | CAMP-dependent protein kinase type I-Alpha, regulatory subunit | PRKAR1A | NM_076598 |
| C50C3.6 | U5 snRNP spliceosome subunit | PRPF8 | NM_066384 |
| CD4.6 | 20S proteasome, regulatory subunit alpha type PSMA1/PRE5 | PSMA1 | NM_072071 |
| Y38A8.2 | 20S proteasome, regulatory subunit beta type PSMB3/PUP3 | PSMB3 | NM_062512 |
| C52E4.4 | 26S proteasome regulatory complex, ATPase RPT1 | PSMC2 | NM_073604 |
| Y49E10.1 | 26S proteasome regulatory complex, ATPase RPT6 | PSMC5 | NM_067208 |
| C23G10.4 | 26S proteasome regulatory complex, subunit RPN2/PSMD1 | PSMD1 | NM_065946 |
| C39F7.4 | GTPase Rab1/YPT1, small G protein superfamily, and related GTP-binding proteins | RAB1A | NM_070996 |
| F10B5.1 | 60s ribosomal protein L10 | RPL10L | NM_063306 |
| T22F3.4 | 60S ribosomal protein L11 | RPL11 | NM_071607 |
| C27A2.2 | 60S ribosomal protein L22 | RPL22 | NM_062531 |
| C09H10.2 | 60S ribosomal protein L44 | RPL36AL | NM_063974 |
| B0250.1 | 60s ribosomal protein L2/L8 | RPL8 | NM_075539 |
| R13A5.8 | 60S ribosomal protein L9 | RPL9 | NM_066259 |
| F54E7.2 | 40S ribosomal protein S12 | RPS12 | NM_065820 |
| C16A3.9 | 40S ribosomal protein S13 | RPS13 | NM_065992 |
| T01C3.6 | 40S ribosomal protein S16 | RPS16 | NM_074289 |
| T05F1.3 | 40S ribosomal protein S19 | RPS19 | NM_060154 |
| C23G10.3 | 40S ribosomal protein S3 | RPS3 | NM_065948 |

Table 1. Cont.

| <i>C. elegans</i> gene symbol | Human gene name | Human gene symbol | Accession number |
|-------------------------------|--|-------------------|------------------|
| B0393.1 | 40S ribosomal protein SA (P40)/Laminin receptor 1 | RPSA | NM_065577 |
| F53E10.6 | RRP15-like protein | RRP15 | NM_071312 |
| VZK822L.1 | Fatty acid desaturase | SCD | NM_001268666 |
| F43D9.3 | Sec1 family domain-containing protein 1 | SCFD1 | NM_001129225 |
| Y113G7A.3 | Vesicle coat complex COPII, subunit SEC23 | SEC23B | NM_075476 |
| Y57E12AL.1 | Tumor differentially expressed (TDE) protein | SERINC1 | NM_171479 |
| T08A11.2 | Splicing factor 3b, subunit 1 | SF3B1 | NM_065452 |
| Y116A8C.42 | Small nuclear ribonucleoprotein Sm D3 | SNRPD3 | NM_070626 |
| ZK652.1 | Small Nuclear Ribonucleoprotein Polypeptide F | SNRPF | NM_066307 |
| T27F2.1 | SNW domain-containing protein 1 | SNW1 | NM_073549 |
| F55A11.2 | SNARE protein SED5/Syntaxin 5 | STX5 | NM_073567 |
| T05C12.7 | Chaperonin complex component, TCP-1 alpha subunit (CCT1) | TCP1 | NM_063321 |
| Y116A8C.35 | U2 small nuclear RNA auxiliary factor 1 isoform b | U2AF1 | NM_070635 |
| C47E12.5 | Ubiquitin-like modifier activating enzyme 6 | UBA6 | NM_001268520 |
| *C46G7.1 | – | – | NM_068504 |
| *F28C6.7a | – | – | NM_063422 |
| *Y105E8C.e | – | – | N/A |
| *K04E7.2 | – | – | NM_076686 |
| *F58G6.7 | – | – | NM_069313 |
| *ZK858.1 | – | – | NM_060045 |
| *Y41D4B.19 | – | – | NM_067703 |
| *F42D1.3 | – | – | NM_078054 |
| *F55C5.4 | – | – | NM_073679 |
| *F17C8.5 | – | – | NM_065572 |
| *C41C4.7a | – | – | NM_063303 |
| *W09B6.1 | – | – | NM_001267098 |
| *D2024.1 | – | – | NM_068750 |
| *W06H8.8 | – | – | NM_001029030 |
| *F25B5.4 | – | – | NM_171139 |

The list consists of the human orthologues of worm genes that, when targeted by RNAi, suppress the paralysis phenotype in A β -expressing worms (n = 78 genes). doi:10.1371/journal.pone.0102985.t001

More generally, the worm screen gene list exhibited a power law distribution such that we could fit a linear regression line (gradient -1.1) to a log-log plot of gene rank bin boundary vs. frequency of observation (Fig. 3, diamonds).

To determine whether the bias is statistically significant we performed a two-tailed Student's t-test [21] to see whether the gradient of the experimental regression line is different from the data generated in the Monte Carlo simulations. A p-value of 0.004

indicates that indeed the hits from our worm screen are more highly interconnected than a comparable random population.

To understand whether such a bias is a common feature of worm RNAi screens, we repeated a similar analysis for three published modifier screens of human neurodegenerative disorders (modelling polyglutamine [22] [Table S2a], tau [23] Table S2b) and alpha-synuclein pathogenesis [24] [Table S2c]) and, congruent with our results, we also found a skew in these screens towards highly interconnected genes (Fig. 4 A–C). Using a one-tailed

Table 2. Enhancers of the A β -paralysis phenotype.

| <i>C. elegans</i> gene symbol | Human gene name | Human gene symbol | Accession number |
|-------------------------------|-----------------|-------------------|------------------|
| W02B8.3 | – | – | NM_064514 |
| F08E10.7 | – | – | NM_075028 |
| F35A5.3 | – | – | NM_076258 |

The list consists of the human orthologues of worm genes that, when targeted by RNAi, enhance the paralysis phenotype in A β -expressing worms (n = 3 genes). doi:10.1371/journal.pone.0102985.t002

Table 3. Gene ontology enrichment for worm screen hits.

| Molecular function |
|---|
| Proton transporting ATP synthase activity, rotational mechanism |
| Proton transporting ATPase activity, rotational mechanism |
| Cellular component |
| Cytosolic small ribosomal subunit |
| Eukaryotic translation initiation factor 3 complex |
| Chaperonin-containing T-complex |
| Biological process |
| Protein binding |
| Structural constituent of ribosome |
| Purine nucleotide binding |

The worm screen hits were analysed for enrichment in molecular function, cellular component and biological process ontology labels.
doi:10.1371/journal.pone.0102985.t003

Student's t-test we observed that for the polyQ ($p = 0.0002$, Fig. 4, panel A), the α -synuclein ($p = 0.04$, panel B), and the tau ($p = 0.04$, panel C) screens, the gradient of the linear regression lines was significantly less than for the Monte-Carlo-generated data. By contrast the equivalent gradient of the GWAS white+grey zone genes was robustly zero ($p = 0.22$, two-tailed, panel D).

The bias toward highly interacting networks in the results of a number of worm modifier screens, including our own, precludes any simple analysis of the overlap between the worm screen and GWAS +1 interactomes. This is because some of the worm genes have several hundred interactors and are likely to generate an overlap by chance. For example HSPA8 constitutes over 30% of the overlap using the hits from our A β screen. For these reasons, we developed a more robust method for determining whether the overlap in the worm and GWAS interactomes was significant or not.

Determining the statistical significance of the overlap between worm screen hits and GWAS results

To compensate for the bias towards highly interacting genes in the worm screen, we designed random Monte Carlo simulations in which each simulated worm +1 interactome has the same size as the particular worm screen gene product being tested.

The statistical significance (p -value) of the overlap between the +1 interactome of each worm screen hit and the GWAS +1 interactome was achieved by generating 1000 random worm +1 interactomes of equivalent size for each experimental worm gene. We then counted how often the overlap of the random worm +1 interactomes with the GWAS +1 interactome was either \geq or \leq to the experimentally observed overlap. To quantify the statistical significance of our findings, we repeated this process for 100 random lists of 60 worm genes.

Overall, we found that, of the 100 random lists of 60 worm genes, 3.14 (95% confidence interval = ± 0.34) genes had +1 interactome overlaps with GWAS that differed significantly from expected at a level of $p < 0.05$. As such, this number is consistent with the random nature of the simulated gene lists. However when we examined the experimental worm screen list, we found that 7 genes had a non-random +1 interactome overlap with the GWAS network. When we reviewed our simulations we found that out of 100 runs only 5 resulted in 7 or more genes that had a +1 interactome overlap that differed from chance, yielding $p = 0.05$ for our observation.

Genes with non-random +1 interactome overlaps

When we considered the overlap between the 7 non-random worm genes we found that 3 (NOP56, PSMA1 and RPL10L; Fig. S5) had a lower +1 interactome overlap with the GWAS list than would be expected by chance. The remaining four worm genes are of particular interest because they have a larger +1 interactome overlap with GWAS than expected. Remarkably, two of these genes (TCP1, CCT8) are components of the TRiC/CCT chaperone complex and the third (MOB4) interacts closely [25,26]. The fourth gene is one of the major folding substrates of the chaperone, namely actin (ACTB). Furthermore, TCP1, CCT8 and MOB4 all interact directly with a single GWAS grey zone gene, namely the kinase STK24 [26] (Fig. 5).

Discussion

Genome-wide association studies [1,13,14] and a subsequent targeted genotyping screen [15] have shown that none of the genes implicated in FAD carry common variants that confer risk for the sporadic version of the disease. These results have called into question the validity of using familial AD, where the pathogenesis is undoubtedly related to A β generation, as a model for the more common sporadic AD. In particular, it is possible that the sporadic disease may have a distinct pathogenesis, perhaps based on immune dysregulation, that is not based on aberrant APP metabolism and the consequent production of A β . To address this issue, we have employed an invertebrate model system that exclusively reports the toxicity of A β ; that is, a worm expressing A β under the control of a muscle-specific driver. While, in this particular model system, the paralysis is likely to be caused by muscle damage, rather than neurodegeneration, it is known that A β toxicity can be observed across a wide range of cell types and the mechanisms may well be conserved.

The worm screen in this study has reported on worm gene transcripts that, when targeted by RNAi, modify the A β -induced paralysis phenotype. The deployment of *rol-6* as a marker of A β expression means that we can rule out any marked artefactual loss of the expression array in response to RNAi. However, we did not measure expression levels of the A β peptide in response to each RNAi treatment, so we cannot exclude the possibility that for a particular RNAi treatment that effects on paralysis could be attributed to changes in transgene expression rather than an effect on A β toxicity. Furthermore this study can usefully be extended by including worm lines carrying mutant alleles of the genes implicated by the RNAi studies both in mammalian systems and in *C. elegans*.

In this study our goal was to use the results of the worm genetic screen to detect GWAS genes with borderline significance that were nevertheless involved in the pathogenesis of sporadic AD. Our initial, and most stringent, test indicated that none of the genes in the GWAS white or grey zones were identical to the human orthologues of the 61 worm modifier genes. This negative finding suggests that, at least for the predominantly Caucasian populations in which GWAS studies have been performed, A β toxicity cannot be considered as identical to sporadic AD. Rather the data support the idea that other pathological pathways may be important in the disorder. However, we did observe that 6 worm gene orthologues were predicted to interact physically with members of the GWAS white+grey zone gene products (Table 4, asterisks). It was also notable that worm modifier genes were much more likely than chance to have a human orthologue. This involvement of a core and essential and highly conserved genes reflects the profound toxic effect posed by A β .

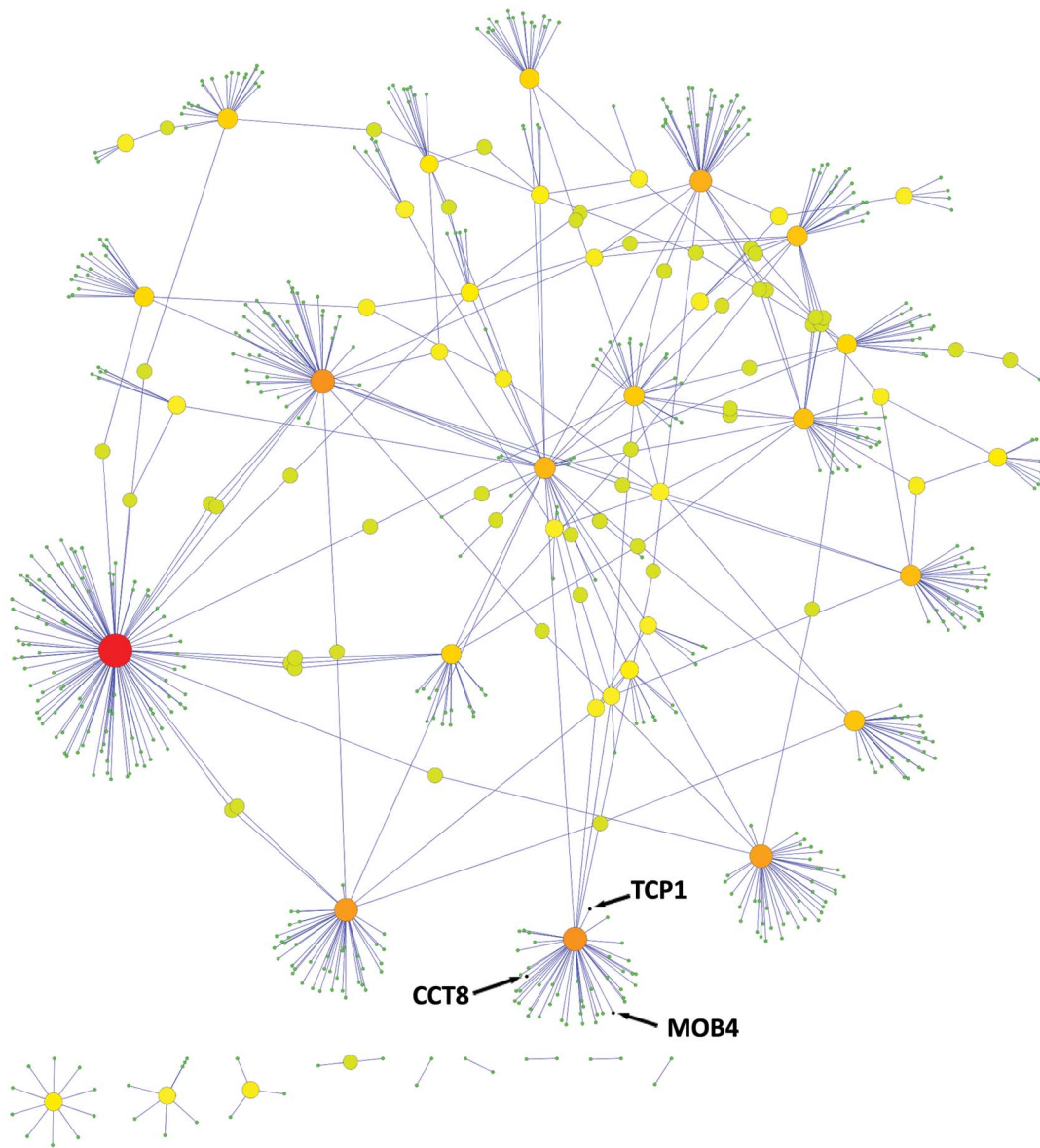


Figure 1. GWAS genes +1 interactome. The +1 interaction network for the 52 GWAS genes with intermediate and high significance ($p < 10^5$). For the 52 genes in the GWAS white+grey zones, there were 703 interactions in the +1 interactome. doi:10.1371/journal.pone.0102985.g001

In order to determine whether the degree of interaction between the worm and GWAS genes was greater, or less, than one would expect by chance we systematically compared the overlap between the worm and GWAS +1 interactomes for each of the worm-screen genes (Fig. S2).

Worm-screen hits, but not the GWAS list, are highly interconnected genes

Considering the +1 interactomes of the worm genes from our $A\beta$ -based screen, we observed that there was a clear bias toward genes encoding highly interactive proteins. As can be seen from Fig. 3, there is a power law relationship between the frequency with which we observe particular gene products and their particular degree of interconnectedness. For our screen, the gradient of the linear fit of the log-log plot is -1.1 . This is significantly different from a gradient of zero, which we observed

for a random set of genes where the chance of observing a gene is independent of its degree of interconnectivity.

We were interested to know whether the gene lists from other genetic screens in worm models of human disease also generated similarly skewed distributions of connectivity. Indeed, when we analysed the data for polyQ, synuclein and tau screens, we found that they all had a negative slope (-1.4 , -0.5 , and -0.4 , respectively) and all were significantly different from the expected zero value.

One possible explanation for the highly interconnected nature of the worm screen hits could be summarised as “sociological bias” [27]. In this context, we hypothesise that previous worm screens have yielded similar gene lists and that the consequent interest in the field has resulted in more interaction data being deposited in the BioGrid database. In support of this hypothesis, we find that the screens for $A\beta$ and polyQ yield 27 common genes, and we find that 20 of them are highly interconnected genes (present in the first

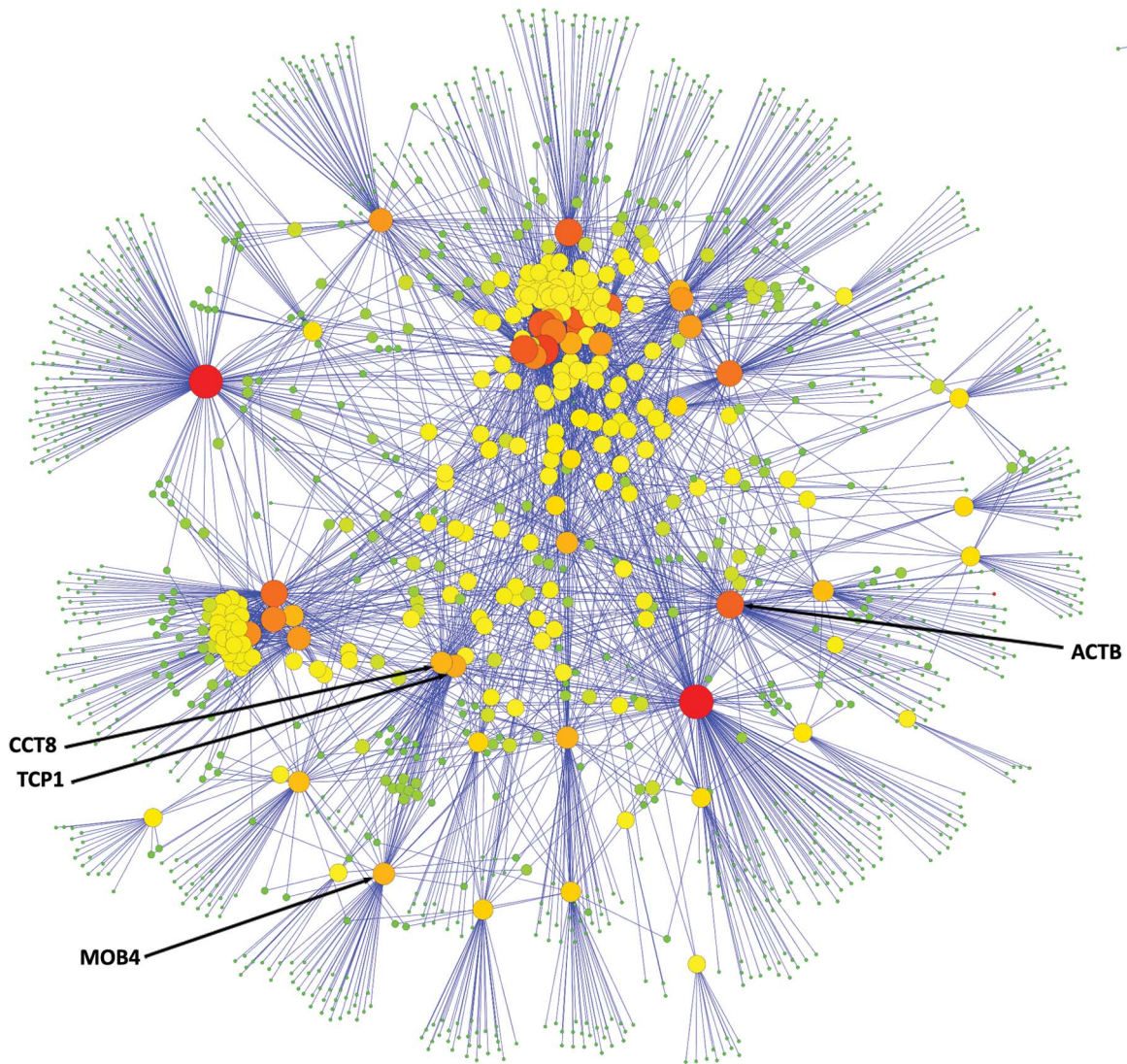


Figure 2. Worm genes +1 interactome. The +1 interaction network for the human orthologues of the 60 worm genes that were highlighted in our worm RNAi screen. For the 60 worm-screen genes with human orthologues, there were 3191 interactions in the +1 interactome. doi:10.1371/journal.pone.0102985.g002

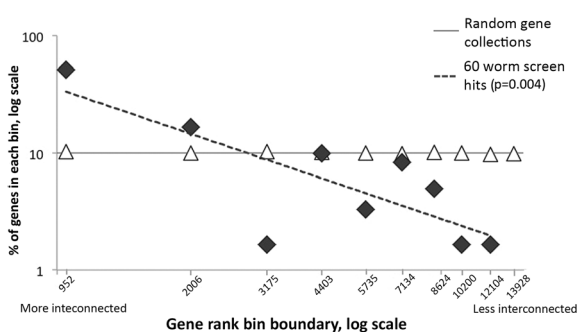


Figure 3. Distribution of rankings of worm genes. The x-axis represents the log of the gene ranking bin boundaries, arranged in decreasing gene-product connectedness from left to right. The y-axis represents the log of the fraction of genes in each bin (where 100% is 60 genes). The dashed line shows the linear regression for the worm screen results. The results of the screens are shown as black diamonds and results of random simulations are shown as empty triangles. doi:10.1371/journal.pone.0102985.g003

bin in plots in Figs. 3 & 4). Even if there is such a sociological bias, this does not invalidate subsequent conclusion because we have carefully compensated for differences in network connectivity.

Another explanation is that genetic modifiers of worm phenotypes really do have more highly interconnected protein products as compared to the average gene [28]. Highly interconnected gene products are likely involved in more biological pathways than less connected ones; so it may be that highly interconnected gene products are more likely to influence disease-related processes as assessed by a genetic screen. However this cannot explain why there is no similar interconnectivity bias when the same analysis is applied to the GWAS white+grey zone genes. Indeed, the distribution of connectivity of the products of white+grey zone genes is remarkably similar to that of the general population of genes. This is likely to be explained by the presence of many false-positive genes in this list.

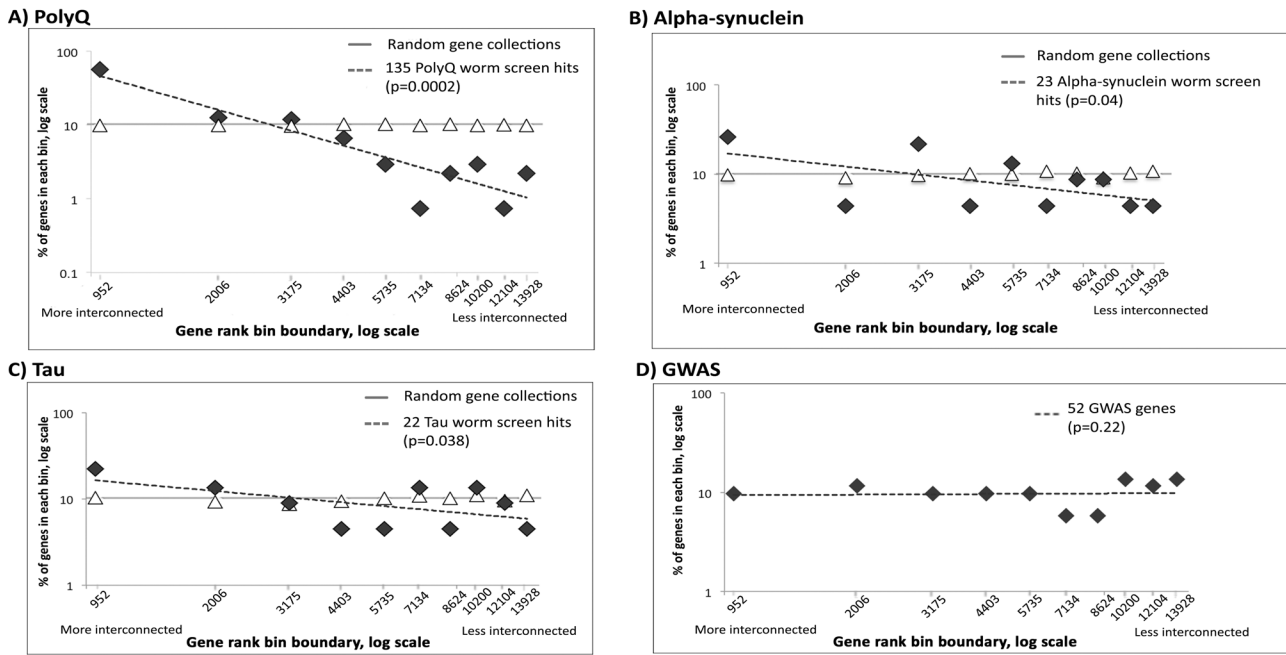


Figure 4. Distribution of rankings of worm models of neurodegenerative diseases. The x-axis represents the log of the gene ranking bin boundaries, arranged in decreasing gene-product connectedness from left to right. The y-axis represents the log of the fraction of genes in each bin (where 100% is 135, 23, 22 & 52 genes for panels A, B, C & D respectively). The dashed line shows the linear regression for the worm screen results. The results of the screens are shown as black diamonds and results of random simulations are shown as empty triangles. (A) polyglutamine screen; (B) α -synuclein screen; (C) tau screen; (D) GWAS candidate white+grey zone genes for AD. doi:10.1371/journal.pone.0102985.g004

Worm-GWAS overlap analysis implicates the TRiC/CCT chaperone in mediating A β toxicity in sporadic Alzheimer’s disease

For each gene in the worm-screen hit list we estimated whether its interactome overlapped with the GWAS interactome to a greater or lesser extent than would be expected by chance. We employed a Monte Carlo simulation approach where we generated 1000 random interactomes that were the same size as the experimental interactome (Fig. S3) and determined the

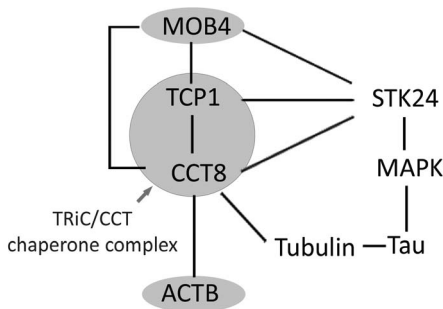


Figure 5. The interaction network of 4 significant worm gene products. Four human orthologues of worm screen gene products (MOB4, TCP1, CCT8 and ACTB) have +1 interactomes that overlap more than expected with the +1 interactome of the GWAS white+grey gene products. Two of these are components of the abundant cytoplasmic TRiC/CCT chaperone, the third (MOB4) interacts closely and fourth (ACTB), along with tubulin, is an important substrate. TRiC/CCT interacts with STK24 and PP2a to form a complex that regulates the MAPK pathway. This network of interactions may have a bearing on tau phosphorylation and neuronal regeneration. doi:10.1371/journal.pone.0102985.g005

distribution of the overlap scores (Fig. S4). For 7 of the 60 worm genes we found that the overlap differed significantly from the chance expectation.

Three of these genes (NOP56, PSMA1 and RPL10L) have +1 interactome overlaps with GWAS white+grey zone genes that are smaller than one would expect by chance, suggesting that they are artifactual modifiers of the worm phenotype and unlikely to be involved in the human disorder. Consequently, these data should dissuade us from investigating the ribosomal [29] and proteasomal [30] functions of these genes in AD. By contrast, the remaining 4 genes exhibited a greater than expected +1 interactome overlap with the GWAS white+grey zone genes. Furthermore, we found that two of these genes (TCP1, CCT8) are both members of the TRiC/CCT chaperone that has a number of substrates including actin (ACTB is the fourth gene) and tubulin. This chaperone complex was also enriched in the gene ontology analysis of the worm hits (Table 3). CCT8 and MOB4 have not been observed as modifiers in any other worm models of neurodegeneration however TCP1 and ACTB RNAi also modify polyQ toxicity [22,23,24]. While this may represent conservation of pathological mechanisms between A β and polyQ it may alternatively indicate that TCP1 and ACTB RNAi constructs have non-specific effects in worm model systems. It is notable that TCP1 levels are abnormal in foetal Down’s syndrome [31]. Furthermore TCP1, CCT8 and MOB4 all interact with each other and also with the kinase STK24, a member of the GWAS grey zone, that has been linked to axonal regeneration in rats [32]. These three candidate genes, along with STK24 and PP2A, form a multiprotein complex that may regulate the MAPK pathway [33]. From our analysis, we propose that both neuroregenerative pathways linked to STK24 and also the MAPK-linked phosphorylation of proteins such as tau [34] may be the mechanisms by which the TRiC/CCT chaperone exerts its effects in AD.

Table 4. Overlap between the +1 interactome for the products of genes in the GWAS white+grey zone and those of genes in the +1 interactome of the worm RNAi screen.

| Gene | p-value | +1 interactome overlap [experimental vs MC] |
|---------------|--------------|---|
| MOB4 | 0.003 | larger* |
| PSMA1 | 0.014 | smaller |
| TCP1 | 0.014 | larger* |
| NOP56 | 0.014 | smaller |
| CCT8 | 0.015 | larger* |
| ACTB | 0.018 | larger |
| RPL10L | 0.033 | smaller |
| RPL9 | 0.058 | smaller |
| ATP6V1B2 | 0.064 | smaller |
| HSPA8 | 0.065 | larger |
| RPL22 | 0.087 | smaller |
| PSMB3 | 0.089 | smaller |
| RPL11 | 0.097 | smaller |
| RPS13 | 0.12 | smaller |
| PSMC2 | 0.131 | smaller |
| PSMD1 | 0.137 | smaller |
| PRPF8 | 0.141 | smaller* |
| ACTR2 | 0.153 | larger |
| ACTG1 | 0.159 | larger* |
| PLRG1 | 0.168 | smaller |
| SCFD1 | 0.189 | smaller |
| AP1M1 | 0.196 | smaller |
| RRP15 | 0.199 | larger |
| U2AF1 | 0.199 | smaller |
| RPS12 | 0.233 | smaller |
| SNW1 | 0.253 | larger |
| RPSA | 0.272 | smaller |
| ARCN1 | 0.289 | smaller |
| SCD | 0.289 | larger |
| ATP5B | 0.299 | larger |
| RPS19 | 0.31 | smaller |
| RPS16 | 0.313 | smaller |
| DARS | 0.314 | smaller |
| RPL8 | 0.322 | smaller |
| STX5 | 0.33 | smaller |
| POLR2A | 0.331 | smaller |
| GSPT2 | 0.333 | larger |
| EIF3G | 0.334 | larger |
| DNAJC3 | 0.343 | smaller |
| PSMC5 | 0.346 | smaller* |
| CPSF2 | 0.362 | smaller |
| SEC23B | 0.371 | larger |
| RAB1A | 0.382 | smaller |
| SF3B1 | 0.421 | smaller |
| PRKAR1A | 0.435 | smaller |
| RPS3 | 0.437 | smaller |
| OGDHL | 0.449 | larger |
| SNRPD3 | 0.458 | smaller |
| ACSF2 | 0.467 | larger |

Table 4. Cont.

| Gene | p-value | +1 interactome overlap [experimental vs MC] |
|-----------|---------|---|
| NDUFA6 | 0.486 | larger |
| UBA6 | 0.515 | larger |
| CRNKL1 | 0.535 | larger |
| MAT1A | 0.539 | smaller |
| RPL36AL | 0.55 | larger |
| ATP6V1A | 0.557 | larger |
| SERINC1 | 0.577 | larger |
| EIF2B5 | 0.58 | smaller |
| HIST1H2BA | 0.58 | smaller |
| AP152 | 0.655 | smaller |
| ATP6VOC | 0.759 | larger |

The human AD GWAS white+grey zone genes, and their +1 interactors, overlap with the human orthologues of worm-screen hits, and their +1 interactors. Worm screen genes that have human orthologues with a significantly non-random +1 interactome overlap with the GWAS list are shown in bold. Worm screen genes that have human orthologues that interact directly with GWAS genes are marked with an asterisk.
doi:10.1371/journal.pone.0102985.t004

The details of the role for TRiC/CCT in AD are unknown; however the finding that RNAi knockdown in the worm protects against A β -induced paralysis indicates that the chaperone in some way mediates A β toxicity. TRiC has been shown to remodel oligomeric protein aggregates in a worm model of polyQ toxicity, with a concomitant reduction in toxicity [35]. It is therefore surprising that knock down TRiC components is protective in our model of A β toxicity, however there are a number of precedents for a reduction of chaperone activity having a protective effect (see [36–42]) and it is hypothesised that low levels of misfolded proteins may induce, or help maintain, the activity of regenerative pathways. Our additional finding that actin RNAi is also protective in the worm screen may indicate that reducing the levels of this important substrate for TRiC/CCT promotes the ability of the chaperone to interact with STK24 and so promote neuroregeneration.

Conclusions

In summary, the lack of a direct overlap between genes implicated by the GWAS studies and the hits from our modifier screen in *C. elegans* indicates that AD cannot simply be considered synonymous with A β toxicity. However using a +1 interactome network approach we have shown that the experimental pattern of overlap between worm and GWAS gene products was significantly non-random. Of those worm genes that showed increased overlap with GWAS lists, three are part of an abundant cytoplasmic complex with important chaperone activity; the fourth gene coded for β -actin that is an important substrate of the same chaperone. The interaction that the TRiC/CCT chaperone has with tubulin, STK24 and the MAPK pathway may explain how A β promotes tau-linked cytoplasmic pathology.

Methods

C. elegans strains

The *C. elegans* strain CL4176 [*smg-1(cc546ts)* dvIs27(pAF29 Pmyo-3::A β 42+pRF4)], expressing A β in body-wall muscle, and the non-A β expressing control, CL802 [*smg-1(cc546ts)* *rol-6(su1006)*] have been described previously [43]. The worms were routinely cultured at the permissive temperature of 16°C on solid

peptone nematode growth media (NGM) as described previously [44].

RNA interference (RNAi) treatment of *C. elegans*

Clones of HT115 *E. coli* carrying RNAi expression plasmids from the whole-genome *C. elegans* feeding library (Geneservice, UK) were cultured separately, in 500 μ l LB medium containing 50 μ g/ml ampicillin, overnight at 37°C. A control culture, carrying empty plasmids without an RNAi insert, was grown simultaneously under identical conditions. Bacteria were seeded drop-wise onto solid NGM plates, supplemented with 25 μ g/ml carbencillin and 1 mM IPTG, and incubated overnight at room temperature. Worm embryos were harvested from synchronised worms as described previously [45] and transferred to NGM agar plates seeded with RNAi-expressing, or control, bacteria and left 48 h to develop into L3 larvae. A β expression was then induced by increasing the ambient temperature to 23°C for 24 h, when the worms were scored for the incidence of the paralysis phenotype.

Primary screen to detect RNAi modifiers of A β -induced paralysis

The interaction of each RNAi-expressing clone with the A β paralysis phenotype in the worm was assessed in triplicate and compared with triplicate wells of worms fed with control bacteria carrying an empty vector. Each plate also had a well containing bacteria expressing RNAi to *unc-22* that normally results in uncoordinated body wall twitching. As a quality control, any plate in which the *unc-22* RNAi-fed worms failed to twitch was discarded and the experiment was repeated.

Locomotor behaviour was assessed at two time-points following the increase in ambient temperature. The first assay was performed 22 h post-induction, at which time A β -expressing worms fed control bacterial cultures were all moving normally. When all worms in each of the triplicate wells for a particular RNAi clone at this time point were seen to be paralysed, then the clone was defined as an enhancer of A β toxicity. This enhancement was specific to A β -expressing worms as no similar paralysis was seen in the corresponding treatment of non-A β -expressing CL802 worms. Clones that non-specifically paralyse worms were not considered. The second time-point, at 32 hr, permitted the detection of suppressors of the paralysis phenotype. At this time-

point, A β -expressing worms under control conditions were all paralysed and so any RNAi-expressing clone that protected the locomotor function of all the worms, in triplicate wells, was defined as a suppressor of A β toxicity.

Secondary screen to confirm the RNAi modifiers of A β -induced paralysis

The secondary screen consisted of a further three experiments, each performed in triplicate wells, for each hit from the primary screen. Paralysis curves were generated by hourly observation of locomotor behaviour and were analysed using Kaplan-Meier plots with statistical significance being estimated using the Mantel-Cox Log Rank test (GraphPad, Prism); $p < 0.05$ was considered significant.

Finding human orthologues of worm genes

According to our pre-planned study design, we considered only those genes in *C.elegans* that have one or more human orthologues. We used the EnsemblCompara phylogenetically based orthology prediction method (<http://www.ensembl.org/>) [17] to find human orthologues of worm genes with minimum 25% amino acid identity [46] with respect to the query gene product. In cases where there was more than one human orthologue, then the gene with the highest % identity was chosen. In approximately 15% of cases one worm gene had multiple human orthologues all with the same percent identity; in these cases, the preferred orthologue was chosen using MetaPhOrs (<http://orthology.phylomedb.org/>) [47] where the consistency score for any orthology was used as the tie-breaker. This score is 1 where an orthology is supported by all the available databases and decreases as agreement is less consistent.

Using this method, human orthologues for 61 out of 78 worm genes were found. The human orthologues of this series of worm genes was then compared with the GWAS white+grey zone genes (Fig. S2.1) as published at the Database of Genotype and Phenotype (dbGaP) of the National Center for Biotechnology Information [48] (http://www.ncbi.nlm.nih.gov/projects/gapplusprev/sgap_plus.htm, $p < 10^{-5}$, Disease = "Alzheimer Disease", access date June 2013).

Network Generation

The "GWAS +1 interactome" consists of all the GWAS white+grey zone genes plus all the genes encoding proteins with which their products physically interact. The "worm +1 interactome" was generated in a similar manner, using 61 human orthologues of the worm modifier screen "hits". The list of interactions was retrieved from the "Biogrid" database (<http://thebiogrid.org>, v. 3.2.96) [19]. The statistical significance of the overlap between the worm +1 interactome and the GWAS +1 interactome was determined by Monte Carlo simulation [49].

Monte Carlo simulations

To test whether any particular worm screen hit g had a +1 interactome that overlapped more with the GWAS +1 interactome than expected by chance, we used the following computational algorithm (Fig. S2):

1. The size of the +1 interactome for each human orthologue of the worm screen hits was determined.
2. Random +1 interactomes, of the same size as the network in step 1, were then generated (Fig. S3). This was achieved by randomly choosing one of the 7970 human orthologues of worm genes, and then generating its +1 interactome and using

this list to progressively populate a random +1 interactome. Once this random list had reached the required length, the process was terminated. If, however, the first randomly selected human orthologue of a worm gene had insufficient interactors to completely populate the required random +1 interactome, then additional random genes and their associated interactor lists were added until the random list was complete.

3. The generated set of random genes was compared with the +1 interactome of the GWAS white+grey zone genes and the number of identical genes was counted (the overlap).
4. Steps 2–3 were repeated 1000 times, yielding a Monte Carlo set of 1000 overlap scores.
5. The number of times that the random overlap was equal to, or greater, than the experimental overlap was counted - this was termed $n_{right,g}$ (Fig. S4, panel A)
6. Similarly the number of times that the random overlap was equal, or less, than the experimental score was also counted - this was termed $n_{left,g}$ (Fig. S4, panel B)
7. We divided either $n_{right,g}$ or $n_{left,g}$, whichever was smaller, by the number of simulations ($n = 1000$) to give the p-value for the overlap (Fig. S2), thus ensuring that a one-tailed test was simulated.

Supporting Information

Figure S1 Paralysis timecourse following induction of A β expression. Increasing the ambient temperature to 23°C when the worms are 48 h old (stage L3) induces A β expression and results in progressive paralysis in worms fed on *E. coli* containing empty vector (a, round symbols). By contrast, a typical suppressor clone rescues this locomotor deficit (square symbols). The paralysed worms (b, arrows) are straighter and largely immobile whereas non-paralysed worms exhibit a marked "roller" phenotype (c, arrowheads), but otherwise move normally. (TIF)

Figure S2 Computational pipeline for determining the significance of the overlap between the +1 interactomes of worm-screen hits and GWAS white+grey zone genes. The algorithm is described more fully in the "Monte Carlo simulations" section of the methods section. (TIF)

Figure S3 Generation of equivalent random +1 interactomes. An illustration of how random +1 interactomes (right) were generated to compare with the +1 interactomes of each of the worm screen hits. Random +1 interactomes were generated containing the same number of genes (in this example, $n = 11$). Human orthologues of worm-screen hits are labeled with "1" (left). Random human genes with a worm orthologue are labeled with "2" (right). Human +1 interactors are represented by small green dots. (TIF)

Figure S4 Estimating the significance of highly overlapping/poorly overlapping +1 interactomes. The +1 interactome of the human orthologues of worm screen genes may overlap more than expected (panel A, contributing to n_{right}) or less than expected (panel B, contributing to n_{left}). Generation of 1000 random +1 interactomes allows the p value for the experimental +1 interactome to be derived. Further details can be found in the "Monte Carlo simulations" section of the methods section. (TIF)

Figure S5 Venn diagram indicating the degree of the +1 interactome overlap for GWAS white+grey genes and each of the significant genes from the worm screen.

Seven genes from the worm screen have human orthologues that have +1 interactomes that overlap more or less than one would expect by chance with the GWAS +1 interactome. Four overlap more (left panel), and three less (right panel), than expected. The area of each circle or overlap is proportional to the number of genes. Worm screen genes that have human orthologues that interact directly with GWAS white+grey zone gene products are marked with asterisks.

(TIF)

Table S1 The 63 human genes in the AD GWAS white+grey zones.

(DOCX)

References

- Lambert J-C, Ibrahim-Verbaas CA, Harold D, Naj AC, Sims R, et al. (2013) Meta-analysis of 74,046 individuals identifies 11 new susceptibility loci for Alzheimer's disease. *Nat Genet* 45: 1452–1458.
- Gatz M, Pedersen NL, Berg S, Johansson B, Johansson K, et al. (1997) Heritability for Alzheimer's disease: the study of dementia in Swedish twins. *J Gerontol A Biol Sci Med Sci* 52: M117–25.
- Gatz M, Reynolds CA, Fratiglioni L, Johansson B, Mortimer JA, et al. (2006) Role of genes and environments for explaining Alzheimer disease. *Arch Gen Psychiatry* 63: 168–174.
- Goate A, Chartier-Harlin MC, Mullan M, Brown J, Crawford F, et al. (1991) Segregation of a missense mutation in the amyloid precursor protein gene with familial Alzheimer's disease. *Nature* 349: 704–706.
- Selkoe DJ (2001) Alzheimer's disease: genes, proteins, and therapy. *Physiol Rev* 81: 741–766.
- Hardy J, Selkoe DJ (2002) The amyloid hypothesis of Alzheimer's disease: progress and problems on the road to therapeutics. *Science* 297: 353–356.
- Rovelet-Lecrux A, Hannequin D, Raux G, Le Meur N, Laquerrière A, et al. (2006) APP locus duplication causes autosomal dominant early-onset Alzheimer disease with cerebral amyloid angiopathy. *Nat Genet* 38: 24–26.
- Schupf N, Patel B, Pang D, Zigman WB, Silverman W, et al. (2007) Elevated plasma beta-amyloid peptide Aβ₄₂ levels, incident dementia, and mortality in Down syndrome. *Arch Neurol* 64: 1007–1013.
- Borchelt DR, Thinakaran G, Eckman CB, Lee MK, Davenport F, et al. (1996) Familial Alzheimer's disease-linked presenilin 1 variants elevate Aβ₄₂/Aβ₄₀ ratio in vitro and in vivo. *Neuron* 17: 1005–1013.
- Jonsson T, Atwal JK, Steinberg S, Snaedal J, Jonsson PV, et al. (2012) A mutation in APP protects against Alzheimer's disease and age-related cognitive decline. *Nature* 488: 96–99.
- Jensen M, Schröder J, Blomberg M, Engvall B, Pantel J, et al. (1999) Cerebrospinal fluid Aβ₄₂ is increased early in sporadic Alzheimer's disease and declines with disease progression. *Ann Neurol* 45: 504–511.
- Harold D, Abraham R, Hollingworth P, Sims R, Gerrish A, et al. (2009) Genome-wide association study identifies variants at CLU and PICAM associated with Alzheimer's disease. *Nat Genet* 41: 1088–1093.
- Lambert J-C, Heath S, Even G, Campion D, Sleegers K, et al. (2009) Genome-wide association study identifies variants at CLU and CR1 associated with Alzheimer's disease. *Nat Genet* 41: 1094–1099.
- Hollingworth P, Harold D, Sims R, Gerrish A, Lambert J-C, et al. (2011) Common variants at ABCA7, MS4A6A/MS4A4E, EPHA1, CD33 and CD2AP are associated with Alzheimer's disease. *Nat Genet* 43: 429–435.
- Gerrish A, Russo G, Richards A, Moskvina V, Ivanov D, et al. (2012) The role of variation at AβPP, PSEN1, PSEN2, and MAPT in late onset Alzheimer's disease. *J Alzheimers Dis* 28: 377–387.
- Kamath RS, Fraser AG, Dong Y, Poulvin G, Durbin R, et al. (2003) Systematic functional analysis of the *Caenorhabditis elegans* genome using RNAi. *Nature* 421: 231–237.
- Flicek P, Ahmed I, Amode MR, Barrell D, Beal K, et al. (2013) Ensembl 2013. *Nucleic Acids Res* 41: D48–55.
- Hillier LW, Coulson A, Murray JI, Bao Z, Sulston JE, et al. (2005) Genomics in *C. elegans*: so many genes, such a little worm. *Genome Res* 15: 1651–1660.
- Chatr-Aryamontri A, Breitkreutz B-J, Heinicke S, Boucher L, Winter A, et al. (2013) The BioGRID interaction database: 2013 update. *Nucleic Acids Res* 41: D816–23.
- Metropolis N, Ulam S (1949) The Monte Carlo method. *J Am Stat Assoc* 44: 335–341.
- Fisher RA (1970) Statistical methods for research workers. Edinburgh Oliver Boyd.
- Nollen EAA, Garcia SM, van Haften G, Kim S, Chavez A, et al. (2004) Genome-wide RNA interference screen identifies previously undescribed

Table S2 Worm RNAi modifiers for screens of various disease models. The genes that modified fly phenotypes when targeted with RNAi are listed for a) polyglutamine, b) tau and c) α-synuclein.

(DOCX)

Acknowledgments

We thank Dr Chris Link for kindly providing the Aβ-expressing worm strains and for helpful discussions. We also thank Florian Hoffelder for his support of this project and Prof Steve Russell for helpful discussions.

Author Contributions

Conceived and designed the experiments: DAL DBS DCC. Performed the experiments: AM DCC DBS. Analyzed the data: EK SJM JW SGO GF DCC. Wrote the paper: EK AM GF DCC. Read the manuscript and gave feedback: EK AM SJM JW DAL SGO GF DBS DCC.

- regulators of polyglutamine aggregation. *Proc Natl Acad Sci U S A* 101: 6403–6408.
- Kraemer BC, Burgess JK, Chen JH, Thomas JH, Schellenberg GD (2006) Molecular pathways that influence human tau-induced pathology in *Caenorhabditis elegans*. *Hum Mol Genet* 15: 1483–1496.
- van Ham TJ, Thijssen KL, Breiding R, Hofstra RMW, Plasterk RHA, et al. (2008) *C. elegans* Model Identifies Genetic Modifiers of α-Synuclein Inclusion Formation During Aging. *PLoS Genet* 4(3): e1000027. doi:10.1371/journal.pgen.1000027.
- Cong Y, Baker ML, Jakana J, Woolford D, Miller EJ, et al. (2010) 4.0-Å resolution cryo-EM structure of the mammalian chaperonin TRiC/CCT reveals its unique subunit arrangement. *Proc Natl Acad Sci U S A* 107: 4967–4972.
- Goudreau M, D'Ambrosio LM, Kean MJ, Mullin MJ, Larsen BG, et al. (2009) A PP2A phosphatase high density interaction network identifies a novel striatin-interacting phosphatase and kinase complex linked to the cerebral cavernous malformation 3 (CCM3) protein. *Mol Cell Proteomics* 8: 157–171.
- Chen J, Aronow BJ, Jegga AG (2009) Disease candidate gene identification and prioritization using protein interaction networks. *BMC Bioinformatics* 10: 73.
- Goh K-I, Cusick ME, Valle D, Childs B, Vidal M, et al. (2007) The human disease network. *Proc Natl Acad Sci U S A* 104: 8685–8690.
- Gautier T, Bergès T, Tollervey D, Hurt E (1997) Nucleolar KKE/D repeat proteins Nop56p and Nop58p interact with Nop1p and are required for ribosome biogenesis. *Mol Cell Biol* 17: 7088–7098.
- Coux O, Tanaka K, Goldberg AL (1996) Structure and functions of the 20S and 26S proteasomes. *Annu Rev Biochem* 65: 801–847.
- Yoo BC, Fountoulakis M, Dierssen M, Lubec G (2001) Expression patterns of chaperone proteins in cerebral cortex of the fetus with Down syndrome: dysregulation of T-complex protein 1. *J Neural Transm Suppl*: 321–334.
- Lorber B, Howe ML, Benowitz LI, Irwin N (2009) Mst3b, an Ste20-like kinase, regulates axon regeneration in mature CNS and PNS pathways. *Nat Neurosci* 12: 1407–1414.
- Zhou TH, Ling K, Guo J, Zhou H, Wu YL, et al. (2000) Identification of a human brain-specific isoform of mammalian STE20-like kinase 3 that is regulated by cAMP-dependent protein kinase. *J Biol Chem* 275: 2513–2519.
- Lambourne SL, Sellers LA, Bush TG, Choudhury SK, Emson PC, et al. (2005) Increased tau phosphorylation on mitogen-activated protein kinase consensus sites and cognitive decline in transgenic models for Alzheimer's disease and FTDP-17: evidence for distinct molecular processes underlying tau abnormalities. *Mol Cell Biol* 25: 278–293.
- Behrends C, Langer CA, Boteva R, Böttcher UM, Stemp MJ, et al. (2006) Chaperonin TRiC promotes the assembly of polyQ expansion proteins into nontoxic oligomers. *Mol Cell* 23: 887–897.
- Lapierre LR, De Magalhaes Filho CD, McQuary PR, Chu C-C, Visvikis O, et al. (2013) The TFE8 orthologue HLH-30 regulates autophagy and modulates longevity in *Caenorhabditis elegans*. *Nat Commun* 4: 2267.
- Taylor RC, Dillin A (2013) XBP-1 is a cell-nonautonomous regulator of stress resistance and longevity. *Cell* 153: 1435–1447.
- Russell RC, Tian Y, Yuan H, Park HW, Chang Y-Y, et al. (2013) ULK1 induces autophagy by phosphorylating Beclin-1 and activating VPS34 lipid kinase. *Nat Cell Biol* 15: 741–750.
- Riedel CG, Down RH, Lourenco GF, Kirienko N V, Heimbucher T, et al. (2013) DAF-16 employs the chromatin remodeller SWI/SNF to promote stress resistance and longevity. *Nat Cell Biol* 15: 491–501.
- Guisbert E, Czyz DM, Richter K, McMullen PD, Morimoto RI (2013) Identification of a Tissue-Selective Heat Shock Response Regulatory Network. *PLoS Genet* 9(4): e1003466. doi:10.1371/journal.pgen.1003466.
- van Oosten-Hawle P, Porter RS, Morimoto RI (2013) Regulation of organismal proteostasis by transcellular chaperone signaling. *Cell* 153: 1366–1378.

42. Kirstein-Miles J, Morimoto RI (2013) Ribosome-associated chaperones act as proteostasis sentinels. *Cell Cycle* 12: 2335–2336.
43. Link CD (1995) Expression of human beta-amyloid peptide in transgenic *Caenorhabditis elegans*. *Proc Natl Acad Sci U S A* 92: 9368–9372.
44. Brenner S (1974) The genetics of *Caenorhabditis elegans*. *Genetics* 77: 71–94.
45. Strange K, Christensen M, Morrison R (2007) Primary culture of *Caenorhabditis elegans* developing embryo cells for electrophysiological, cell biological and molecular studies. *Nat Protoc* 2: 1003–1012.
46. Lechner M, Findeiss S, Steiner L, Marz M, Stadler PF, et al. (2011) Proteinortho: detection of (co-)orthologs in large-scale analysis. *BMC Bioinformatics* 12: 124.
47. Prysycz LP, Huerta-Cepas J, Gabaldón T (2011) MetaPhOrs: orthology and paralogy predictions from multiple phylogenetic evidence using a consistency-based confidence score. *Nucleic Acids Res* 39: e32. doi:10.1093/nar/gkq953.
48. Mailman MD, Feolo M, Jin Y, Kimura M, Tryka K, et al. (2007) The NCBI dbGaP database of genotypes and phenotypes. *Nat Genet* 39: 1181–1186.
49. Besag J, Clifford P (1991) Sequential Monte Carlo p-values. *Biometrika* 78: 301–304.